Industrial Engineering Letters
ISSN 2224-6096 (Paper) ISSN 2225-0581 (online)
Vol.3, No.6, 2013

Numerical and Experimental Investigation of Co-Shedding Vortex Generated by Two Adjacent Circular Cylinders and Its Effect on Air Flow Behaivor around Naca 2412 Airfoil

Hayder Kraidi RASHID NASRAWI
Babylon University, College of Engineering, Department of Mechanics, Iraq
E-Mail: hayderkraidi@yahoo.com

Abstract
The vortex shedding effect on flow separation around airfoil NACA 2412 was investigated. To control the location of separation point, the turbulent flow was generated. To induce turbulent pattern, flow was disrupted by two adjacent circular cylinders in upstream of airfoil with 10 mm diameter for each cylinder. An experimental technique based on smoke wind tunnel with different air flow velocities (1.7 m/s and 2.5 m/s) was provided. The conjunction between the effect of the angles of attack and flow visualization around the airfoil NACA 2412 was verification. The angles of attack (0, 5 and 10) degree was used for each air flow velocity. ANSYS program software used to simulate and comparison all the experimental results. The experimental and numerical results showed, when the angle of attack increase, the location of the separation point was shifted toward the airfoil NACA 2412 leading edge. Also, effect of the wake of two cylinders on the location of the separation point was very clear. The vortex induced beyond the cylinders and upstream the airfoil help to prevent separation growth, thereby, the turbulent provided will accelerated the flow around the airfoil geometry and the adverse pressure in that location was decreased. So, the increases in airflow velocity will help the turbulent boundary layer to growth. The growth of turbulent flow boundary layer tends to avoid separation and the flow will reattached. Moreover, the accuracy of results were checked by validation the Kutta-condition experimentally and numerically.
Keywords: Boundary layer control, airfoil NACA 2412, flow visualization, smoke wind tunnel

Nomenclature
Cp = pressure coefficient
D=cylinder diameter 10mm
p = pressure, N/m2
Re=Reynolds number
u, v = velocity components in boundary layer in x and y direction respectively , m/s
V= average velocity m/s
x, y = cartesian coordinates

Greek symbols
α =angle of attack deg.
ρ=air flow density kg/m^3
μ= viscosity N.m/s

Subscript
D=cylinder diameter
c=airfoil chord

1. Introduction

There are many manners to generate turbulent flow like change the flow velocity, using heat generation, increase the roughness of the surface and flow disrupted as done in this research . In order to get turbulent flow, two adjacent circular cylinders are used as flow obstruction. This position of cylinders will produce co-shedding vortices and this mean, fluctuation in flow stream line, this will lead to produce turbulent flow. The flow turbulent intensity will change by using different flow velocities. The turbulent flow is used to improve the location of the separation point. Where, in turbulent boundary layer the stagnation point near the airfoil surface will accelerate the flow and converted separation point to slip down even may be past the airfoil body. Moreover, The laminar boundary layer can be detached easier compare with turbulent one from the airfoil surface. Many researchers studied the effect of turbulent flow (numerically and experimentally) on the airfoil flow visualization, for example Albert Q.(2002) experimented the location of flow separation over NACA 2412 airfoil and gives a stall location as a function of angle of attack. Small smoke wind tunnel was used to predict the stall location with flow speed (1.6 m/s) corresponding to cord Reynolds number 8900 at angles of attack (4, 6, 8 and 10) degree. The results show that the stall location will progress rapidly toward the leading edge when the angle of attack increase and there is a wide difference between the separation points on the upper and underneath surface of airfoil NACA2412 for each angle of attack. Many researchers produced suitable methods to control flow by

generation vortex or turbulent flow inside or in front of airfoil Christopher L. Rumsey and Takafumi Nishino (2011) presented three numerical codes to simulate two dimensional circulation control flow over airfoil (large-eddy simulation LES code and two Reynolds-averaged Navier–Stokes RANS codes). The effects of different turbulence models was investigated. A comparison between incompressible and compressible flow solvers was produced. Also, reported that all Reynolds-averaged Navier–Stokes computations produce higher circulation than large eddy simulation computations with different stagnation point location and greater flow acceleration around the nose onto the upper simulation surface. Sanjay Mittal and Priyank Saxena (2002) used stabilized finite element formulations to solve the incompressible, Reynolds averaged Navier–Stokes equations in conjunction with the Baldwin–Lomax model. They observed that the separation point over stationary airfoil NACA 0012 moves gradually towards the leading edge with the increasing angle of attack. Shutian Deng et al (2007) investigated the effects of different unsteady blowing jets on the surface of airfoil NACA 0012 at the location just before the separation points. They found that the length of separation bubble is significantly reduced (almost removed) after unsteady blowing technology is applied. Hua Shan et al (2008) presented the numerical simulation of subsonic flow separation over a NACA0012 airfoil with a 6^o angle of attack and flow separation control with vortex generators. They modeled both the passive and active vortex generators using the immersed-boundary method. They observed that the passive vortex generators can partially eliminate the separation by reattaching the separated shear layer to the airfoil over a significant extent. Salam H.(2005) presented a suitable theoretical research for control flow around the airfoil NACA 0012. Also, the effect of rotating circular cylinder on the boundary layer acceleration around the surface of airfoil NACA 0012 was produced. This circular cylinder placed in front of the airfoil with angles of attack (0°,5°,10°,14° and 20°) respectively. The results show that, the turbulent flow generated by rotating circular cylinder has a benefit on the boundary layer reattached. Seifert (1996) experiment the effect of the roughened airfoil to generate turbulent flow on the location of separated point. Many works were done to investigate the flow separation over airfoil and how to dominate on this complex phenomena like Stefan Schmidt and Frank Thiele (2004) carried out the flow around the A-airfoil at maximum lift (α = 13.3◦) and Re = 2×10^6 using numerical simulation depends on RANS and DES to quantify the influence of transient flow patterns on the quality of the flow prediction. C. M. Rhie and W. L. Chow (1983) described the turbulent floe using the k-ε model. Donghyun You (2007) using LES as numerical method to simulation the flow over an airfoil at a high angle of attack and to verification the pressure gradients, turbulent boundary layers, wakes, and flow separation so as to flow control. Imad Shukry Ali and Sahab Shehab Ahmed (2011) using (k-ε) turbulent model in order to numerical simulation for the separation flow of a 2D, incompressible, steady and turbulent flow around (NACA 0012) airfoil. Rong Ma and Peiqing Liu (2009) presented the numerical simulation of low-Reynolds-number and high-lift airfoils. The FLUENT computational software used for numerical simulation. Dr.Sabri Tosunoglu et al (2010) verification the circulation over airfoil and focusing on the Kutta-Zhukowsi condition and observed the future of the strong of vortex to move the rear stagnation point to the trailing edge. Also, they studied the characteristics of airfoil and experiment many conditions in order to formulate the inverse design procedure to design and improve a winglet. Most of researchers reports that Reynolds number, airfoil angle of attack, airfoil shape and pressure distribution are the main characteristic of flow separation. In order to control flow separation from airfoil surfaces, the turbulent flow generation is the simplest. The problem was how to get the best and simplest way to generate turbulent flow and the technology using of this type of flow in suitable position to reduce the bad effect of flow separation .The objective of this work is to investigate the flow control over unsymmetrical airfoil NACA 2412 by turbulent generation. The turbulent flow over airfoil was accomplished by co-shedding vortex that induced by mounting two adjacent circular cylinder in flow upstream as shown in figure (1) part a. Moreover, the flow separation location change by turbulent flow effect was verification .The stagnation point generated at leading airfoil edge with and without the two cylinders was observed experimentally and theoretically. The complex behavior analysis of flow in the regime vicinity of the two adjacent circular cylinders and airfoil leading edge was Performed figure(1) part b, and will explained in subsequent articles. The effect of change of the cylinders diameter, and the critical space between two cylinders wall and the airfoil leading edge, will presented in next paper. In order to check the accuracy of theoretical and experimental solution, the Kutta-condition at rear airfoil was satisfy in both experimental and theoretical work, the airfoil NACA2412 and the cusped trailing edge of this airfoil shown in figure (2).Although that the turbulent flow is time depended [9], the solution emphases on the onset generation of turbulent flow.

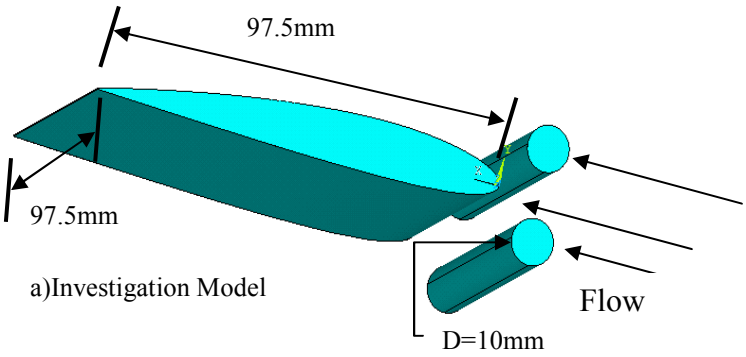

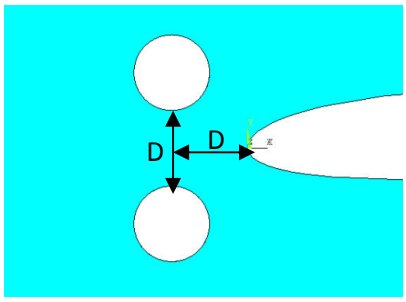

b) Co-shedding vortex flow generated region.

Figure (1): NACA 2412 airfoil with two circular cylinder upstream.

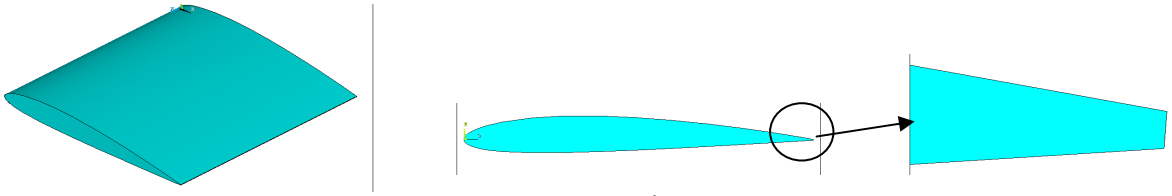

Figure (2):NACA 2412 airfoil a) general shape, b) side view, c) the finite trailing edge.

2. Grid generation

The numerical flow simulation is satisfy using ANASYS (11) package to solution of flow problems. The commercial softwer (ANSYS) built on finite element method (FEM). The approximation of the (FEM) depends on the type of mesh generation and size of element cell.There are two types of mesh generation , structure mesh and unstructure mesh where the types of mesh depends on the feacher of points connectivity. In structure mesh the connection is regular compare with unstructure mesh.The both types of mesh generation is used in this work and can be shown in figure (2). The numerical results accuracy extensive reliance on optimization mesh generation.

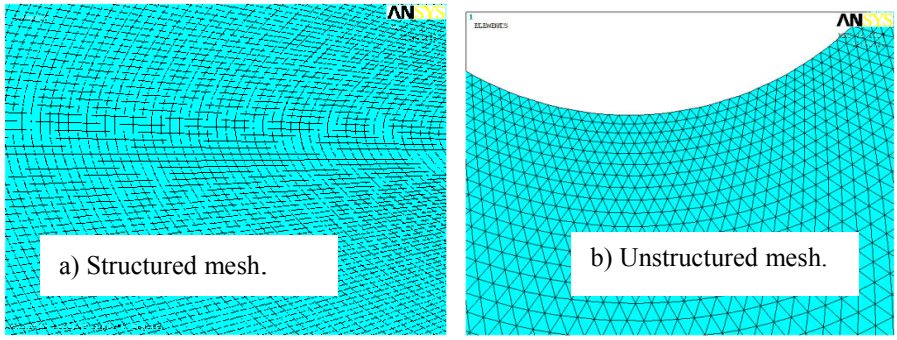

Figure (3): Types of mesh generation.

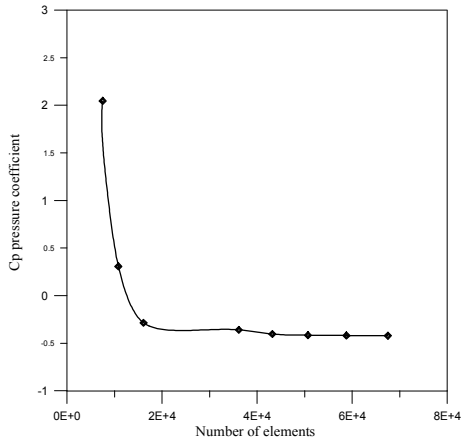

Figure (4): The relation between the number of elements and pressure coefficient.

The optimization mesh generation can predicted by experimented numerically solution of random point until reach to excepted accuracy by increases the number of elements and decreases element size. The pressure iteration convergence reach to 10^{-4} and velocity components u and v iteration convergent until 10^{-6}. The convergence criterion of pressure and velocity component, used to solve continuity and momentum partial differential equations, with stable iteration results is very fine to get accuracy results under relaxation parameter equal to 0.5. The pressure coefficient given by the following relation [14]:

$$Cp = \frac{p - p_\infty}{1/2\rho V^2} \quad \text{.....(1)}$$

Where p_∞ is atmospheric pressure.

In present work the mesh generation divided into two types depends on the complicated of the physical phenomenon. First situation is analyzed the flow characteristic around airfoil NACA 2412 with air flow velocities (1.7 m/s and 2.5m/s) at angles of attack (α=0, 5 and 10 degree), this situation solved numerically depending on the triangle mapping mesh and refined the flow street solely around airfoil section to validates the obtained results in this region. The second situation is flow improved by generate co-shedding vortex beyond two circular cylinder to dominate the flow characteristic around the same unsymmetrical airfoil NACA 2412 with same angles of attack and air flow velocities. The regime vicinity to the two cylinders and the airfoil leading edge is very complex regime. In order to approximate numerical solution of this region used unstructured mesh and the size of cell is very small. Unstructured grids usually consist of a mix of quadrilaterals and triangles in 2D in order to resolve the boundary layers properly [15]. The main reason of the unstructured grids is based on the fact that triangular (2D) grids can be generated automatically, independent of the complexity of the domain [15]. The first situation of mesh generation shown in figure (5), at angles of attack α=0, 5 and 10 degree. The second situation of mesh generation shown in figure (6) , at angles of attack α=0, 5 and 10 degree.

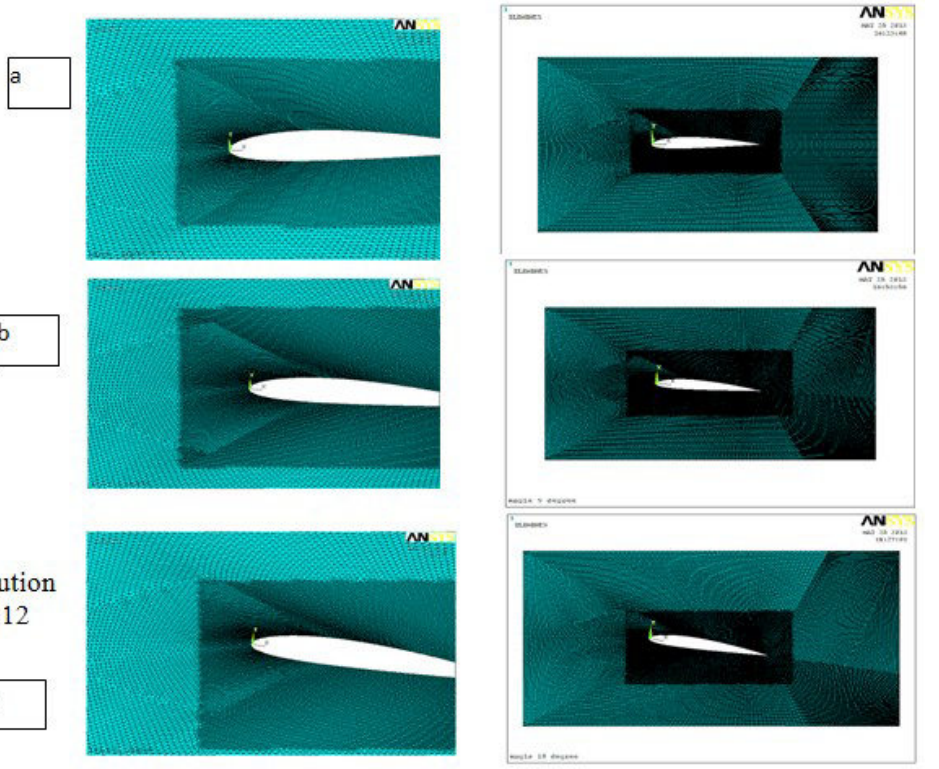

Figure (5) :Mesh distribution around airfoil NACA 2412 a) at α =0°, b) at α =5° and c) at α =10°.

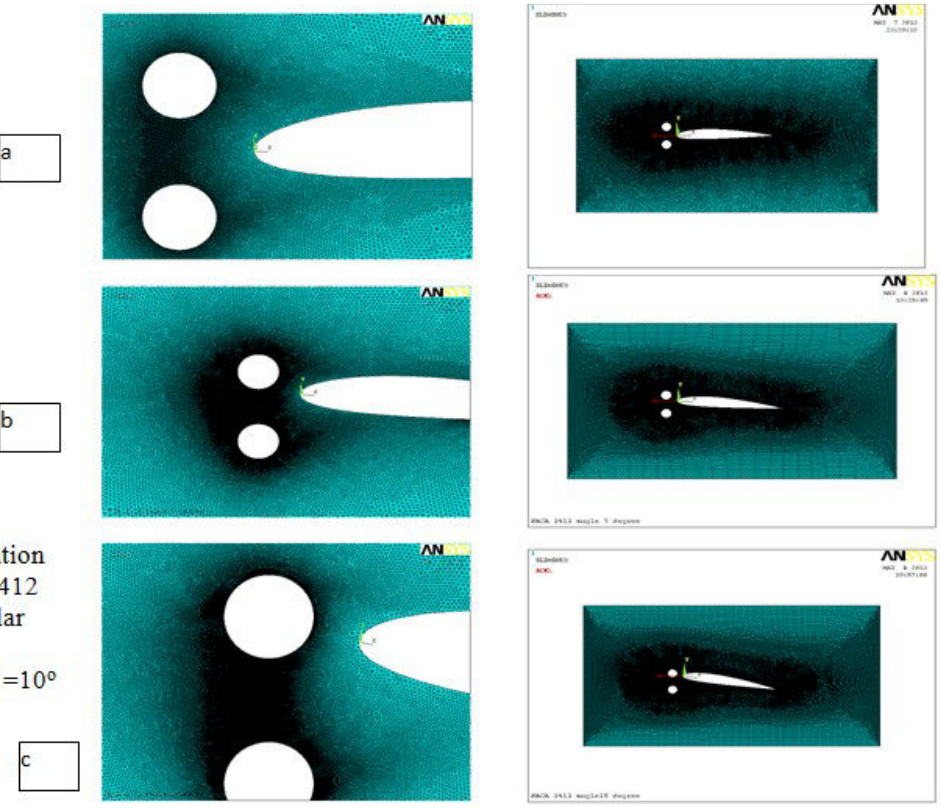

Figure (6): Mesh generation around airfoil NACA 2412 with two adjacent circular cylinder in front at a) α =0°, b) α =5° and c) α =10°

3. Kutta condition at trailing edge of airfoil

Airfoil NACA 2412 is four-digit type. This type of airfoil gives unsymmetrical geometry. The first digit represents the maximum camber as relative to chord. Also, the second one is presented the location of the maximum thickness of the chamber. The last two digits 12 refer to maximum thickness in airfoil section. In this type of airfoil the thickness equation gives a gap as presented figure (2).There two manner to solve this problem ,

the first one is to modified the trailing edge of airfoil or handling the actual trailing edge by satisfy the Kutta-condition. The Kutta-condition states, when the flow leaves the trailing edge of a sharp-tailing airfoil smoothly: that is, the velocity is finite there [16]. For onset turbulent flow generation and without sharp-trailing edge the Kutta condition can be presented by assuming that the wake which was emanates from the airfoil rear is very thin. With this thin wake the circulation sill fixed, this lead to coincides the pressure up and down the airfoil trailing edge, so the flow velocity at trailing edge up and down will be the same. This will satisfy the Kutta-condition [16] and[11]. Figure (7) represent the mesh generation at the airfoil trailing edge with angles of attack 0, 5 and 10 degree.

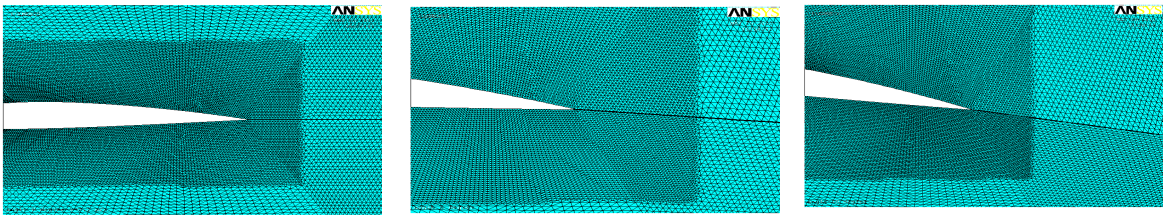

a) b) c)

Figure(7):Mesh generation around the rear of the airfoil NACA 2412 at a)α=0 degree, b) α=5degree and c) α=10 degree.

4. Experimental work

The experimental work based on the smoke wind tunnel shown in figure (8). The atmospheric air is drown through the test section by fan located at apparatus top. The dimensions of the test section are 35.5 cm x 17.8 cm, the section will change to circular with diameter 12.7 cm past the test section near the fan. The fan can operate with variable speed. The experimental models shown in figures (1) and (2) will mounted in test section. Two air flow velocity applied on the experimental models (1.7m/s and 2.5 m/s). For each air flow velocity the angle of attack change from 0^o then 5^o and final 10^o. Camera with 30 frame per sec. is used. However, our study emphases on the onset effect of turbulent generation on flow visualization around the airfoil, in this case the features of camera is sufficient. The flow visualization around the airfoil with different angles of attack is obvious by injection kerosene vapor as white stream line through the air flow. All experimental works were accomplished in Babylon University college of engineering mechanical departments.

Figure(8): Smoke wind tunnel.

5. Theoretical approximation and boundary conditions

In this research the efforts devoted to investigate the influence of the onset turbulent flow on the air flow visualization over airfoil NACA 2412.The new k-ε model is used to analysis the flow around the airfoil NACA 2412 and to analyses the flow behavior over the system consist of the two adjacent circular cylinder with airfoil NACA 2412 behind. The model assumptions can be summarized in the following points:

1. Steady state (onset turbulent flow situation).
2. Incompressible (low air flow velocities).
3. Two dimensional flow.
4. The velocity of flow very close to solid wall, equal to zero (by viscosity effect).
5. The effect of inertia force is greater than the viscosity (will get turbulent flow).

To predict the flow type the Reynolds number was calculated first depends on the cylinder diameter Re_D and the second depends on the airfoil chord Re_C.

$$Re_D=\frac{\rho V D}{\mu} \quad \text{.....(2)}$$

$$\mathrm{Re}_c = \frac{\rho V c}{\mu} \quad \ldots\ldots(3)$$

Where c represent the airfoil chord.

The conservation equation can be summarized as below:

a) Continuity equation [17]&[11].

$$\frac{\partial u}{\partial x} + \frac{\partial v}{\partial y} = 0 \quad \ldots\ldots(4)$$

b)The momentum equations in x-direction[17]&[11].

$$\rho\left(u\frac{\partial u}{\partial x} + v\frac{\partial u}{\partial y}\right) = -\frac{\partial p.}{\partial x} + \frac{\partial}{\partial x}\left(2\mu_{eff}\frac{\partial u}{\partial x}\right) + .\frac{\partial}{\partial y}\left(2\mu_{eff}\frac{\partial u}{\partial y}\right) \quad \ldots\ldots(5)$$

c)The momentum equations in y-direction[17]&[11].

$$\rho\left(u\frac{\partial v}{\partial x} + v\frac{\partial v}{\partial y}\right) = \rho g_y - \frac{\partial p.}{\partial y} + \frac{\partial}{\partial x}\left(2\mu_{eff}\frac{\partial v}{\partial x}\right) + .\frac{\partial}{\partial y}\left(2\mu_{eff}\frac{\partial v}{\partial y}\right) \quad \ldots\ldots(6)$$

where

μ_{eff} = effective viscosity

when the flow is turbulent the velocity in x direction involving the mean component $\bar{u}$ and fluctuation component u' as shown in equation below.

$$u = \bar{u} + u' \quad \ldots\ldots(7)$$

Also, the velocity in y direction involving the mean component $\bar{v}$ and fluctuation component v' as shown in equation (8).

$$v = \bar{v} + v' \quad \ldots\ldots(8)$$

For turbulent flow we get the Reynolds stress(σ) in term of x (σ_x) and y (σ_y) direction that which introduced into momentum equations (5)and (6).

$$\sigma_x = -\frac{\partial}{\partial x}\left(\rho u'u'\right) - \frac{\partial}{\partial y}\left(\rho u'v'\right) \quad \ldots\ldots(9)$$

$$\sigma_x = -\frac{\partial}{\partial x}\left(\rho v'u'\right) - \frac{\partial}{\partial y}\left(\rho v'v'\right) \quad \ldots\ldots(10)$$

Also, an effective viscosity is defined as the sum of the laminar viscosity and the turbulent viscosity:

$$\mu_{eff} = \mu + \mu_t \quad \ldots\ldots(11)$$

In k-ε model the turbulent viscosity is calculated as a function of the turbulence parameters kinetic energy k and its dissipation rate ε.

$$\mu_t = \rho C_\mu \frac{k}{\varepsilon} \quad \ldots\ldots(12)$$

The value of uses both a variable C_μ term and a new dissipation source term. The C_μ function used by the new k-ε model is a function of the invariants. This function found in most of turbulent flow books for more details you can see reference [17].

6. Results and discussion

The flow visualize can be simply illustrated depends on flow stream line. The stream lines were generated by smoke wind tunnel. Where, the stream lines refer to the flow direction, so, the distance between the smoke lines, represent the air flow relative velocities and then the static pressure variation. Figure (9) represent the realistic flow around airfoil NACA 2412 that mounted on test section of smoke wind tunnel at air flow velocity (1.7 m/s) with Re_c=11943 and angle of attack 0^o. As shown in this figure the flow cover all airfoil geometry with very small separation region at the airfoil rear. The reason that the energy of flow would be dissipated at the cusped trailing edge. This experimental results have a good agreement with reference [1]. When the air flow increase to (2.5 m/s) with Re_c=17564 as shown in figure (10), the steam lines separation is very clear at trailing

edge. Since, the flow deceleration starting from airfoil trailing edge by adverse pressure effect. The unsymmetrical shape effect on stream lines deflected observed in figure (9), where the stream lines moves closer when deflection to up surface compare with down surface of airfoil. The lift and drag forces are the main forces acts on the airfoil and have to taken in account with any phenomenon that happen on airfoil. The figures (11,12,13 and 14) illustrated the variation between separation location and angle of attack, where, the separation reign progress towards the airfoil leading edge when the angle of attack increase. The relations between the lift and drag forces contributed to predicted the location of boundary layer detached. Moreover, the increase flow velocity will help the airfoil to generate bigger lift force, but also help to generated separation. In order to avoid this effect, two circular cylinder was proposed to increase flow energy by flow obstruction. The turbulent energy will accelerate flow and help to re-oriented flow and re-attached boundary layer, this shown clearly at figures (15,16,17,18,19 and 20). The features of these figures that the distance between the streamlines in vicinity flow regime behind cylinder and perior airfoil will be closer, this mean the velocity will increase and the static pressure will change to dynamic pressure. Figure (13) shows that at angle of attack 10^o, the flow stream lines will cross each other at airfoil rear and the Kutta condition will not satisfy at this situation, since the flow circulation not equal zero. while, the increase in flow velocity (increase flow energy) will prevent stream line to wrap at trailing edge. In order to validate the results, the experimental results were simulated using ANSYS(11). Figures (21 to 26) illustrated the pressure contour and velocity contour with angles of attack (0^o,5^o and 10^o). The pressure down the airfoil deceleration and acceleration over the airfoil leading edge. The numerical results have very good agreement with experimental one. To check the flow behavior around the airfoil trailing edge the figure (27) presented the Kutta-condition at trailing edge with angles of attack (0^o,5^o and 10^o) with air flow velocity 1.7 m/s as velocity vector. The flow at airfoil rear is very smooth and the relative velocity at up and down trailing edge will be the same, since the circulation equal to zero. For extensive the all results and emphases on the pressure distribution at the leading edge and velocity at the trailing edge the figures(28, 29 and 30). These figures show that the flow at trailing edge with different velocity and different angle of attack stay smooth with steady flow. The features of onset flow the time not taken in account, this lead to handling effect of the co-shedding vortex just generated on flow behavior around the leading airfoil. The figures (31 and 32) illustrated the two cylinders vortex effect on the stagnation point that generated at leading edge with Re_D=1194 at flow velocity (1.7 m/s) and Re_D=1757. The stagnation point will push the flow and boundary layer to reattachment by acceleration the flow around the airfoil leading and slip down the location of separation point towards the airfoil rear. Moreover, the pressure at stagnation point on the leading edge will growth three time with the two circular cylinders than flow without cylinders, since the flow confined between the cylinders and re-directed to airfoil. The increasing in stagnation pressure handling the flow and increase the flow energy. This energy help to accelerate the flow and presumably make the separation more difficult.

7. Conclusions

The aim of this research is to investigate the flow control over NACA 2412 by effect of onset turbulent flow generation. This turbulent flow induced using two adjacent circular cylinder that play as flow obstruction. The conclusions can be summarized in the following :

The disrupted flow increase the ability to control flow around the airfoil and accelerate the flow over the airfoil. Also, the onset turbulent flow gives a sufficient imagination about the flow behavior. Moreover, to predict the Kutta- condition the smoke wind tunnel experimental results can be used. Therefore, the flow control over airfoil located past two adjacent circular cylinder gives a new matter must study in more details, like the effect of cylinders diameter and critical distance between the cylinders system and airfoil leading edge. This research may lead to help to flow control over airfoil without electric or mechanical auxiliary device and with low cost.

8. Refetrences

1]. Albert Q. Einstein, "Flow Visualization of Stall on NACA 2412 Airfoil", Blacksburg, Virg tinia, April (2002).

2]. Christopher L. Rumsey and Takafumi Nishino, " Numerical study comparing RANS and LES approaches on a circulation control airfoi", International Journal of Heat and Fluid Flow 32 (2011) 847–864. www.ivsl.org.iq.

3]. Sanjay Mittal and Priyank Saxena, " Hysteresis in flow past a NACA 0012 airfoil", Comput. Methods Appl. Mech. Engrg. 191 (2002) 2179–2189. www.ivsl.org.iq.

4]. Shutian Deng, Li Jiang, Chaoqun Liu, " DNS for flow separation control around an airfoil by pulsed jets", Computers & Fluids 36 (2007) 1040–1060. www.ivsl.org.iq.

5]. Hua Shan, Li Jiang, Chaoqun Liu, Michael Love and Brant Maines," Numerical study of passive and active flow separation control over a NACA0012 airfoil", Computers & Fluids 37 (2008) 975–992. www.ivsl.org.iq.

6]. Salam H., ” Incompressible Flow Over An Airfoil With Rotating Cylinder”, Ph.D. Thesis, University of Baghdad, (2005).
7]. Sifert, A., Darabi, A. and Wygnanski.I., ”Delay Of Airfoil Stall By Periodic Excitation”, J. aircraft, Vol.33, No.4, pp(691-698), (1996).
8]. Nakasone Y. and Yoshimoto S. and Stolarski T. A., “Engineering Analysis With Ansys Software”, Burlington, MA 01803, (2006).
9]. Stefan Schmidt and Frank Thiele, " Detached Eddy Simulation of Flow around A-Airfoil ″, Flow, Turbulence and Combustion **71:** 261–278, (2003).
10]. C. M. Rhie and W. L. Chow, " Numerical Study of the Turbulent Flow Past an Airfoil with Trailing Edge Separation", AIAA Journal ,Vol. 21, No. 11, November, (1983)
11]. Donghyun You, Frank Ham, and Parviz Moin, "Discrete Conservation Principles in Large-Eddy Simulation with Application to Separation Control over an Airfoil", Physics of Fluids , Volume 20 , Issue 10, special topic: turbulence physics and control—papers from a workshop in honor of john kim's 60th birthday, Stanford, California, September, (2007).
12]. Imad Shukry Ali and Sahab Shehab Ahmed, **"** Modeling of Turbulent Separation Flow", World Academy of Science, Engineering and Technology 76 (2011).
13]. Rong Ma, Peiqing Liu, "Numerical Simulation of Low-Reynolds-Number and High-Lift Airfoil S1223", Proceedings of the World Congress on Engineering (WCE) Vol. I, July 1 - 3, (2009), London, U.K.
14]. Dr. Sabri Tosunoglu, Dr. George S. Dulikravich, Gianluca Minnella, Jose Ugas and Yuniesky Rodriguez," Aerodynamic Shape Design Optimization of Winglets", EML 4905 Senior Design Project, Florida International University, 25 Oct.(2010).
15]. J. Blazek, "Computational Fluid Dynamics: Principles and Applications", *Alstom Power Ltd., Baden-Daettwil, Switzerland*, (2001).
Elsevier Science Internet Homepage
http://www.elsevier.nl (Europe)
http://www.elsevier.com (America)
http://www.elsevier.co.jp (Asia)
16]. J. M. McDonough, "Introductory Lectures on Turbulence", Physics, Mathematics and Modeling Departments of Mechanical Engineering and Mathematics, University of Kentucky (2007).
17].Jack Moran, "An Introduction to Theoretical and Computational Aerodynamics", University of Minnesota, Copyright (1984), by John Wiley & Sons. Inc.

Figure (9): Flow streamline with V=1.7 m/s α=0 deg. Compare with Ref.[1].

Figure (10): Air flow velocity =2.5 m/s α=0 deg.

Figure (11): Air flow velocity =1.7 m/s α=5 deg.

Figure (12): Air flow velocity =2.5 m/s α=5 deg.

Figure (13): Air flow velocity =1.7 m/s α=10 deg. Compare with Ref.[1].

Figure (14): Air flow velocity =2.5 m/s α=10 deg.

Figure (15): Air flow velocity =1.7 m/s α=0 deg.

Figure (16): Air flow velocity =2.5. m/s α=0 deg.

Figure (17): Air flow velocity =1.7 m/s α=5 deg.

Figure (18): Air flow velocity =2.5 m/s α=5 deg.

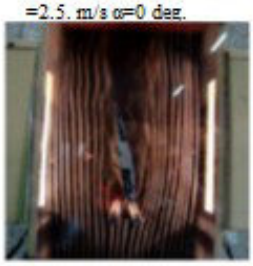

Figure (19): Air flow velocity =1.7m/s α=10 deg.

Figure (20): Air flow velocity =2.5 m/s α=10 deg.

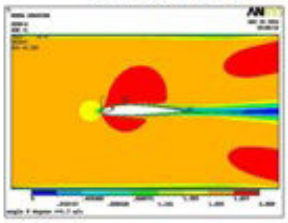

a)Velocity contour at V=1.7 m/s

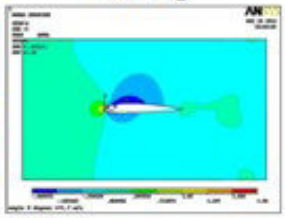

b)Pressure contour at V=1.7 m/s

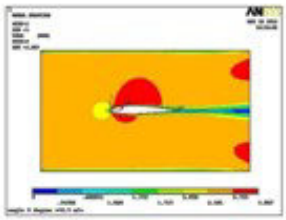

c)Velocity contour at V=2.5 m/s

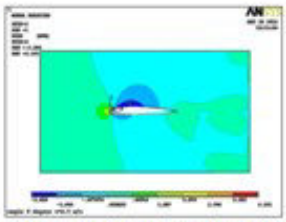

d)Pressure contour at V=2.5 m/s

Figure (21): Pressure and velocity contour at angle of attack $\alpha = 0°$.

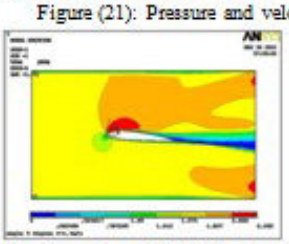

a)Velocity contour at V=1.7 m/s

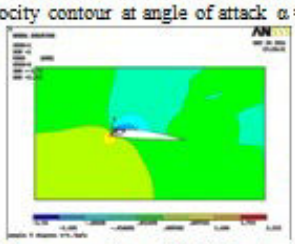

b)Pressure contour at V=1.7 m/s

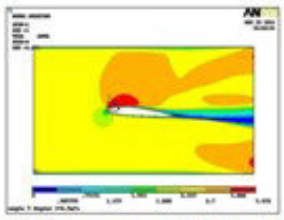

c)Velocity contour at V=2.5 m/s

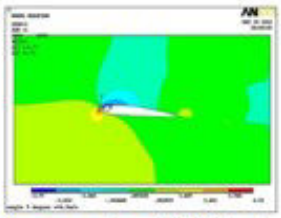

d)Pressure contour at V=2.5 m/s

Figure (22): Pressure and velocity contour at angle of attack $\alpha = 5°$

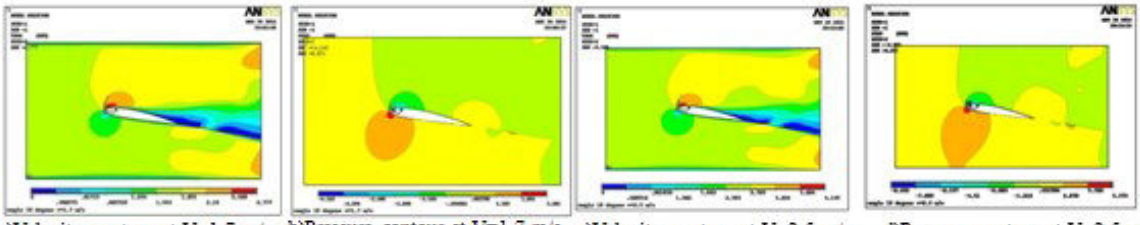

a)Velocity contour at V=1.7 m/s b)Pressure contour at V=1.7 m/s c)Velocity contour at V=2.5 m/s d)Pressure contour at V=2.5 m/s

Figure (23): Pressure and velocity contour at angle of attack $\alpha = 10°$.

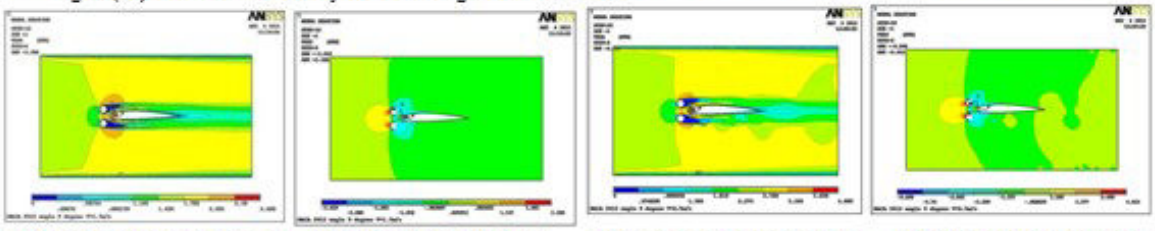

a)Velocity contour at V=1.7 m/s b)Pressure contour at V=1.7 m/s c)Velocity contour at V=2.5 m/s d)Pressure contour at V=2.5 m/s

Figure (24): Pressure and velocity contour with two adjacent circular cylinder at $\alpha = 0°$.

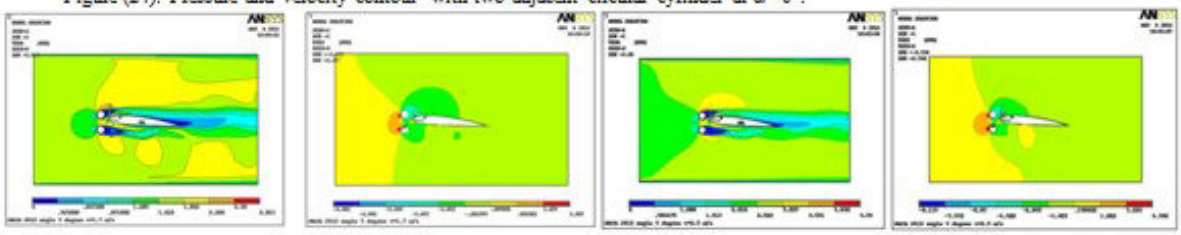

a)Velocity contour at V=1.7 m/s b)Pressure contour at V=1.7 m/s c)Velocity contour at V=2.5 m/s d)Pressure contour at V=2.5 m/s

Figure (25): Pressure and velocity contour with two adjacent circular cylinder at $\alpha = 5°$.

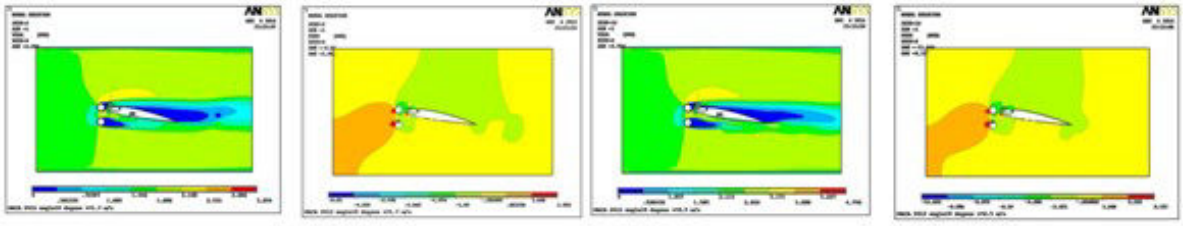

a)Velocity contour at V=1.7 m/s b)Pressure contour at V=1.7 m/s c)Velocity contour at V=2.5 m/s d)Pressure contour at V=2.5 m/s

Figure (26): Pressure and velocity contour with two adjacent circular cylinder at $\alpha = 10°$

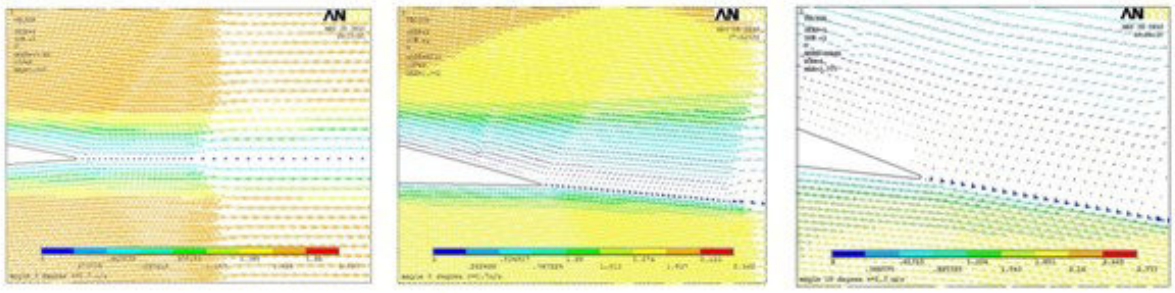

a b c

Figure (27): The part a, b and c represents velocity vector at trailing edge with air flow velocity =1.7 m/s at α=0 °, α=5° and α=10° respectively

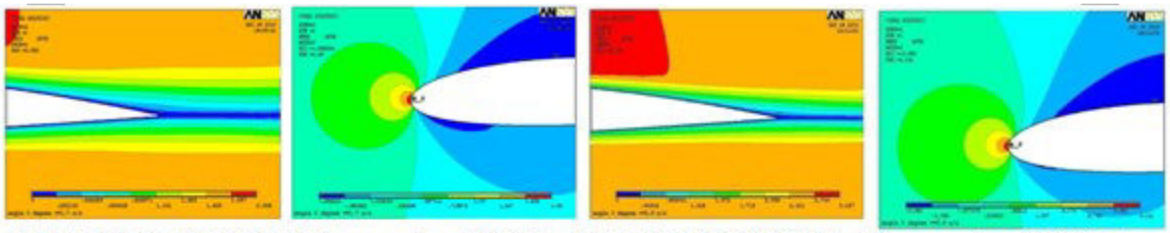

a)Velocity contour at V=1.7 m/s b)Pressure contour at V=1.7 m/s c)Velocity contour at V=2.5 m/s d)Pressure contour at V=2.5 m/s

Figure (28): Pressure and velocity contour with two adjacent circular cylinder at $\alpha = 0°$

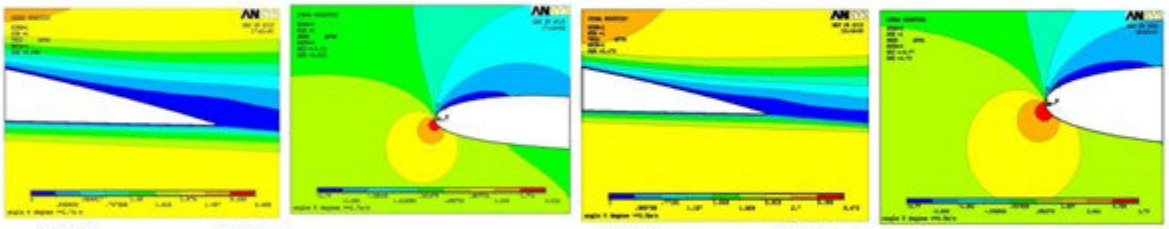

a)Velocity contour at V=1.7 m/s b)Pressure contour at V=1.7 m/s c)Velocity contour at V=2.5 m/s d)Pressure contour at V=2.5 m/s

Figure (29): Pressure and velocity contour with two adjacent circular cylinder at $\alpha = 5°$

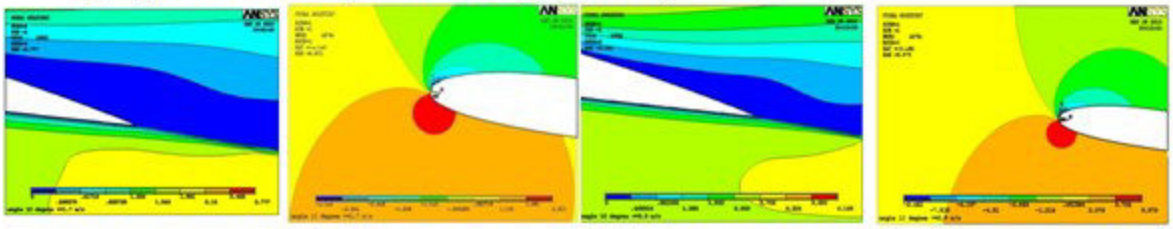

a)Velocity contour at V=1.7 m/s b)Pressure contour at V=1.7 m/s c)Velocity contour at V=2.5 m/s d)Pressure contour at V=2.5 m/s

Figure (30): Pressure and velocity contour with two adjacent circular cylinder at $\alpha = 10°$.

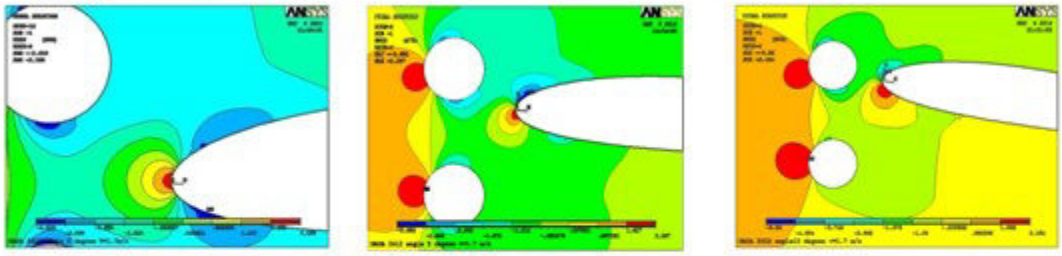

a b c

Figure (31): The part a, b and c represents pressure contour at leading with air flow velocity =1.7 m/s at $\alpha = 0°$, $\alpha = 5°$ and $\alpha = 10°$ respectively .

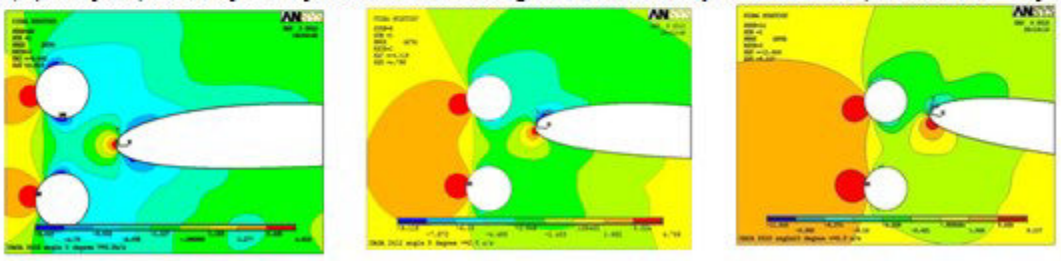

a b c

Figure (32): The part a, b and c represents pressure contour at leading with air flow velocity =2.5 m/s at $\alpha = 0°$, $\alpha = 5°$ and $\alpha = 10°$ respectively .